Т. 10. №6. 2024
https://doi.org/10.33619/2414-2948/103

UDC 621.43.068 https://doi.org/10.33619/2414-2948/103/35

THE ENERGY CIRCUIT OF THE EXHAUST GAS HEAT RECOVERY CIRCUIT OF A 25 KW DIESEL GENERATOR

©Zhou Min, *ORCID: 0009-0009-3107-4225, Jiangsu University of Science and Technology, Ogarev Mordovia State University, Zhenjiang, China, Saransk, Russia, 2281963429@qq.com*
©Kuznetsov D., *SPIN-code: 6451-1920, Ph.D., Ogarev Mordovia State University, Saransk, Russia*

ЭНЕРГЕТИЧЕСКАЯ СХЕМА РЕКУПЕРАЦИИ ВЫХЛОПНЫХ ГАЗОВ ДИЗЕЛЬНОГО ГЕНЕРАТОРА МОЩНОСТЬЮ 25 КВТ

©Чжоу Минь, *ORCID: 0009-0009-3107-4225, Цзянсуский университет науки и технологии, Национальный исследовательский Мордовский государственный университет им. Н.П. Огарева, г. Чжэньцзян, Китай, г. Саранск, Россия, 2281963429@qq.com*
©Кузнецов Д. В., *SPIN-код: 6451-1920, канд. техн. наук, Национальный исследовательский Мордовский государственный университет им. Н.П. Огарева, г. Саранск, Россия*

Abstract. The purpose of the work is to describe the installation using differential equations and obtain approximate values before the experiment. In this paper, a constructive scheme of the experimental device is proposed, and the principle of its operation is described in detail. The power circuit of the device has been drawn up. Complex impedance, frequency function, amplitude-frequency characteristic and phase-frequency characteristic are obtained by mathematical transformation of the power circuit. The frequency response of the circuit is constructed. As a result of the calculations, we will obtain the amplitude frequency response and the phase frequency response. Using the found values of the characteristics, we will build graphs and draw conclusions about how the characteristics depend on the change in parameters and why the graph lines of the graphs are exactly the way they are.

Аннотация. Цель работы — описать установку с использованием дифференциальных уравнений и получить приблизительные значения перед экспериментом. В данной статье предлагается конструктивная схема экспериментального устройства и подробно описан принцип его работы. Составлена схема питания устройства. Комплексный импеданс, частотная функция, амплитудно-частотная характеристика и фазово-частотная характеристика получаются путем математического преобразования силовой цепи. Построена частотная характеристика цепи. В результате расчетов получена амплитудная и фазовая частотные характеристики. Используя найденные значения характеристик построены графики и сделаны выводы о том, как характеристики зависят от изменения параметров и почему линии графов точно такие, какие они есть.

Keywords: waste heat recovery, diesel generator, hydraulic, heat exchanger, heat transfer.

Ключевые слова: восстановление отработанного тепла, дизельный генератор, гидравлика, теплообменник, теплопередача.

At present, the energy problem has become a global issue and is highly valued by countries around the world. Due to the needs of science and technology and economic development, we need more and more energy to supply. At the same time, we are increasingly relying on these energy

Т. 10. №6. 2024
https://doi.org/10.33619/2414-2948/103

sources. Therefore, we must develop reasonably, use it efficiently, and save energy as much as possible. Protect the environment, save energy and reduce emissions while reducing energy use. Diesel engine is one of the most commonly used power devices, but a large amount of waste heat is wasted during use. Research shows that the internal combustion engine can only use about one-third of the total energy released by fuel combustion, and the remaining two-thirds are dissipated in the form of waste heat [1]. In order to make full use of the waste smoke waste heat of the unit, reduce fuel consumption, improve the efficiency of power generation and the comprehensive utilization rate of energy, and reduce the pollution of smoke to the environment, the waste gas waste heat of diesel generators can be recycled as a heat source. The pulse mode is used in the waste heat recovery system to transfer heat more efficiently.

Diesel residual heat recovery is mainly used in vehicles and ships. In recent years, the waste heat recycling technology of internal combustion engines has attracted more and more attention from governments and scholars. In 2009, the EU actively launched the Seventh Framework Action Plan and launched a two-year "HeatReCar" automotive engine waste heat recovery program involving European countries [2]. Cummins [3], AVL [4] and BMW [5] have also carried out research on engine waste heat recovery technology with universities and scientific research institutions. The waste heat resources available to internal combustion engines mainly include engine exhaust waste heat and engine cooling water waste heat [6]. However, because the heat energy quality taken away by cooling water is not high, most of the engine waste heat recovery and utilization technologies are researched on engine exhaust energy. At present, the waste heat recovery and utilization technologies of automotive internal combustion engines mainly include: turbocharged technology, absorption/adsorption refrigeration technology, temperature difference power generation technology and thermal cycle waste heat recovery technology. Among them, turbocharged technology has been applied on a large scale.

In recent years, the technology of recovering engine exhaust waste heat using the Ronken cycle system has attracted widespread attention from scholars at home and abroad, and major research institutions and enterprise colleges around the world have carried out a series of research work on this. In terms of engineering research, Khaliq [7] and others studied the exhaust waste heat of HCCI internal combustion engines based on organic Langken cycle fueled by ethanol. Research shows that the thermal efficiency can reach 41.5% after installing the Ronken cycle system. Tahani M et al. [8] took R-134a, R-123 and R-245fa as the cyclic working mechanism to optimize the two Longken cycle structures that recover the exhaust and cooling water and heat of diesel engines at the same time. In terms of structural research, Kim YM et al. [9] proposed a high-efficiency gasoline engine exhaust waste heat recovery single-loop organic Langken cycle system to recover engine exhaust and coolant waste heat. This structure overcomes the complex structure and space occupancy limit of the dual-circuit system, and increases the power by 20%. Rijpkema J et al. [10] studied the recovery of engine coolant, exhaust and other waste heat under twelve working types using the Langken cycle, cross-critical Langken cycle, triangular flash evapor cycle and first-stage flash cycle.

For the waste heat recovery of marine diesel engines. In March 1979, West Germany KHD cooperated with the Institute of Ship Power Installations of the University of Berlin to carry out experimental research on the waste heat utilization system of large engines. In this experiment, the two teams invested in and manufactured a complete set of power generation equipment needed for the diesel engine exhaust waste heat utilization system. The heat source of the exhaust waste heat is provided by a diesel engine with a power of 1470kW and a rotation speed of 1000rpm. When the diesel engine is rated, the exhaust heat energy accounts for 30% of the total energy, and the continuous provision of heat energy can also be guaranteed under partial loads [11]. Almost at the

Т. 10. №6. 2024
https://doi.org/10.33619/2414-2948/103

same time, Mitsubishi Heavy Industries in Japan developed a new waste heat utilization system (STG). After flowing through the action of the exhaust gas turbine and turbocharger, the exhaust enters the waste heat recovery device, and the resulting steam acts on the output of the steam turbine, steam turbine and runoff exhaust gas turbine.

The work is incorporated into the deceleration gear to drive the generator to generate electricity [12]. China's first 7RTA84TD diesel engine equipped with waste heat utilization system was produced by Dalian Marine Diesel Engine Co., Ltd. The system was simplified on the basis of Wartsila's waste heat utilization system. The power turbine device was abandoned and the steam generated by the waste heat boiler was used to generate electricity or meet the requirements. Daily life services. The system can generate 1100 kW of electricity when the load is greater than 55%. At present, it has been successfully installed on the VLCC manufactured by Bochuan Heavy Industries and is used by Singapore Global Shipping Company [13].

In this paper, it is proposed to recover the waste heat of diesel generators in the form of pulsation. Differential equations are used to describe the process of hydraulic and heat transfer. In order to describe the process, we first establish an energy circuit, compile the equation, set the input and output through the black box, calculate the equation with the black box, write the image equation, compile the complex resistance equation, distinguish coefficient, write the frequency function of the energy circuit, distinguish between the real part and the virtual part of the complex resistance, and calculate the amplitude frequency and phase frequency characteristics. Finally, a graph is established according to the calculation of amplitude frequency and phase frequency characteristics, and conclusions are drawn from the graph.

Unit Description for Simulation

The principle of operation of the experimental setup Figure 1 shows an experimental installation of a waste heat exchanger with a phase change.

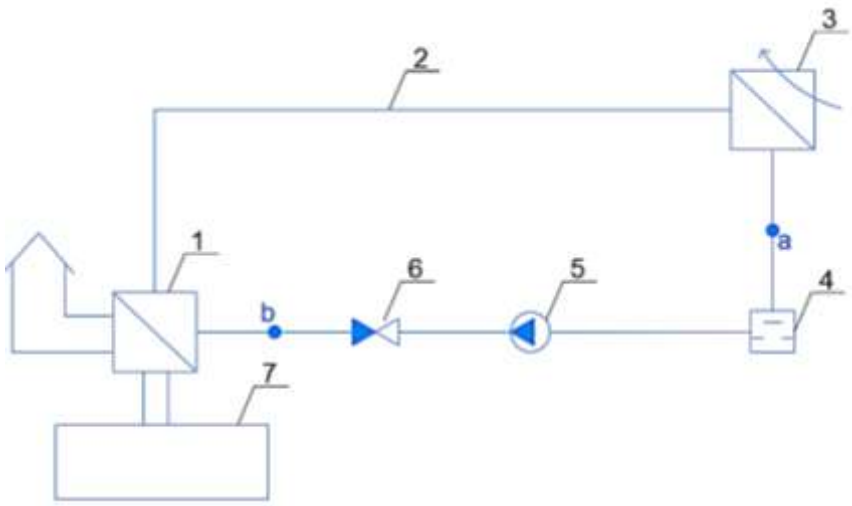

Figure 1. Experimental device for the recycling loop: 1 ~ Heat exchanger; 2 ~ Pipeline; 3 ~ Heat exchanger; 4 ~ Shock valve; 5 ~ Pump; 6 ~ Check valve; 7 ~ Diesel generator

The exhaust gases of the diesel generator 7 passing through the heat exchanger of the heat exchanger 1 give off heat to the heated water (coolant). The coolant circulates in the hot water circuit due to the pump 5. After turning on the pump 5, the coolant moves along the circuit: check valve 6, heat exchanger utilizer 1, pipeline 2, heater 3, shock valve 4. When the coolant flow rate reaches a set (for example 2 m/s), the shock valve will quickly close and the kinetic energy of the flow before it turns into a potential one accompanied by an increase in pressure (point a). When the pressure at point a reaches its maximum, a reverse wave will form that will go in the opposite

direction to point B. When the high-pressure wave passes through the colorizer 3 and the heat exchanger heat exchanger 1, it will increase heat transfer.

In the course of the study, for a better understanding of the scheme, it was decided to study 2 characteristics of hydraulic and thermal, in order to better understand the nature of the forces arising and to more accurately determine the required parameters on the obtained model.

The first is hydraulic, which takes into account elastic properties of a spring with pliability *l* (pliability is the inverse of elasticity), inertial properties of a liquid by mass *m*, pressure losses in the pipeline by means of active resistance *r*. The third part is the network pump, and inertial properties of a liquid by mass m_2.

In the first power circuit the hydraulic characteristics at the moment of closing of the shock valve is considered. This circuit contains 2 elements.

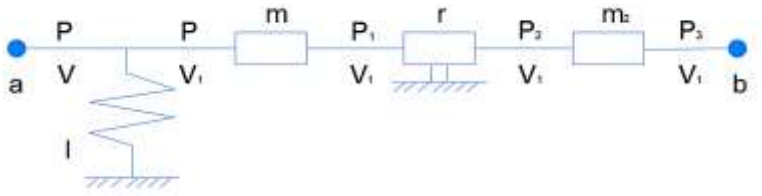

Figure 2. Hydraulic circuit

The circuit link equations:

$$\begin{cases} P=m\dot{V}_1+rV_1^2+m_2\dot{V}_1+P_3 \\ V=l\dot{P}+V_1 \end{cases}$$

Black box:

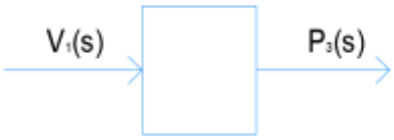

Figure 3. Black box for hydraulic energy circuit

Equations for P_3: $P_3=P_{30}+\overline{P}_3$
Equations for V_1: $V_1=V_{10}+\overline{V}_1$
Equation for V_1^2: $V_1^2\approx V_{10}^2+2V_{10}\overline{V}_1$
Equation for P:

$$P=m\dot{\overline{V}}_1+rV_1^2+m_2\dot{\overline{V}}_1+P_3=m\dot{\overline{V}}_1+r(V_{10}^2+2V_{10}\overline{V}_1)+m_2\dot{\overline{V}}_1+P_{30}+\overline{P}_3=$$
$$m\dot{\overline{V}}_1+rV_{10}^2+2rV_{10}\overline{V}_1+m_2\dot{\overline{V}}_1+P_{30}+\overline{P}_3$$

Equation for $\dot{\overline{P}}$: $\dot{\overline{P}}=m\ddot{\overline{V}}_1+2rV_{10}\dot{\overline{V}}_1+m_2\ddot{\overline{V}}_1+\dot{\overline{P}}_3$
Equation for V:

$$V=l\dot{P}+V_1=l\left(m\ddot{\overline{V}}_1+2rV_{10}\dot{\overline{V}}_1+m_2\ddot{\overline{V}}_1+\dot{\overline{P}}_3\right)+V_{10}+\overline{V}_1$$
$$=(lm+lm_2)\ddot{\overline{V}}_1+2rlV_{10}\dot{\overline{V}}_1+\overline{V}_1+V_{10}+l\overline{P}_3=b_3\dot{\overline{P}}_2+a_1\ddot{\overline{V}}_1+a_2\dot{\overline{V}}_1+a_3\overline{V}_1+a_4+b\dot{\overline{P}}_3$$

Equation for images:

$$(a_1s^2+a_2s+a_3)V_1(s)=-bP_3(s)$$

Т. 10. №6. 2024
https://doi.org/10.33619/2414-2948/103

Coefficients:

$$a_1=lm+lm_2$$
$$a_2=2rlV_{10}$$
$$a_3=1$$
$$a_4=V_{10}$$
$$b=1$$

Complex circuit resistance $Z(s)$:

$$Z(s)=\frac{P_3(s)}{V_1(s)}=\frac{a_1s^2+a_2s+a_3}{-b}$$

Frequency function of the circuit:

$$s\rightarrow j\Omega,\ j^2=-1$$

Frequency function of the circuit:

$$Z(j\Omega)=\frac{a_1\Omega^2-a_2j\Omega-a_3}{b}$$

The real part of the frequency function:

$$Re(j\Omega)=\frac{a_1\Omega^2-a_3}{b}$$

Imaginary part of the frequency function:

$$Im(j\Omega)=\frac{-a_2\Omega}{b}j$$

Amplitude-frequency response (frequency response) of the circuit:

$$A(j\Omega)=\sqrt{Re(j\Omega)^2+Im(j\Omega)^2}$$

Phase frequency response (FFC) of the circuit:

$$\varphi(j\Omega)=-arctg\frac{Im(j\Omega)}{Re(j\Omega)}$$

Figure 4 shows the part of the installation where heat transfer takes place.

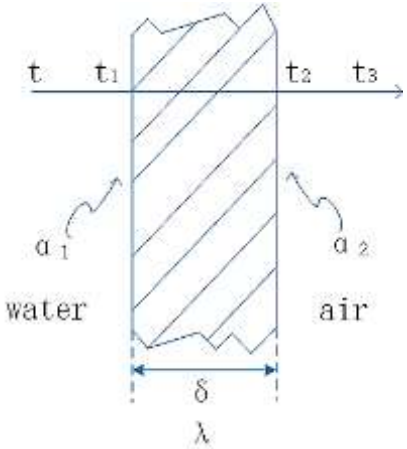

Figure 4. Part of the heat transfer plant: t – the temperature of hot water; t_1, t_2 – wall temperature; t_3- the temperature of the air; α_1 – convective heat transfer coefficient of water and left wall; α_2 – convective heat transfer coefficient of air and right wall; δ – the thickness of the wall surface; λ – Thermal conductivity of the wall

Т. 10. №6. 2024
https://doi.org/10.33619/2414-2948/103

When the hot water flows, the convective heat transfer coefficient between the water and the left wall is h_1, and the temperature of t is greater than t_1, so the wall absorbs the heat brough by the hot water, and the wall temperature rises. When the temperature rises to t_1, the surface temperature of the left wall is stable. The thickness of the wall is λ, and the heat is transmitted from the left wall to the right wall by means of heat conduction. When the temperature rises to t_2, the surface temperature of the right wall reaches a stable state. The right wall carries out convective heat transfer with the air, and the convective heat transfer coefficient is h_2. Through convective heat transfer, heat is transferred to the air until the air temperature t_3 reaches a stable state.

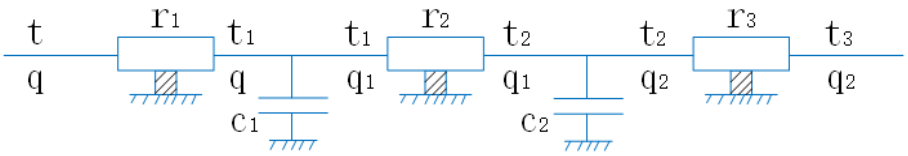

Figure 5. Heat transfer energy circuit

The circuit link equations:

$$\begin{cases} t=r_1q+r_2q_1+r_3q_2+t_3 \\ q=c_1\dot{t}_1+c_2\dot{t}_2+q_2 \end{cases}$$

The input and output of the energy chain for thermal calculation are presented in the form of a “black” box.

Figure 6. Black box for heat transfer

Equations for $t_3, t_2, \dot{t}_2, t_1, q_2$:

$$t_3=t_{30}+\bar{t}_3$$

$$t_2=r_3q_2+t_3$$

$$\dot{t}_2=\dot{\bar{t}}_2=r_3\dot{\bar{q}}_2+\dot{\bar{t}}_3$$

$$t_1=r_2q_1+t_2$$

$$q_2=q_{20}+\bar{q}_2$$

Equations on q_1 from the 1st link:

$$\begin{gathered} q_1=c_2\dot{t}_2+q_2 \\ =c_2\left(r_3\dot{\bar{q}}_2+\dot{\bar{t}}_3\right)+q_{20}+\bar{q}_2 \\ =c_2r_3\dot{\bar{q}}_2+c_2\dot{\bar{t}}_3+q_{20}+\bar{q}_2 \end{gathered}$$

Equations on t_2 from the 1st link:

$$t_2=r_3q_2+t_3=r_3q_{20}+r_3\bar{q}_2+t_{30}+\bar{t}_3$$

The equation on t_1:

Т. 10. №6. 2024
https://doi.org/10.33619/2414-2948/103

$$t_1=r_2q_1+t_2$$
$$=r_2\left(c_2r_3\dot{\bar{q}}_2+c_2\dot{\bar{t}}_3+q_{20}+\bar{q}_2\right)+\left(r_3q_{20}+r_3\bar{q}_2+t_{30}+\bar{t}_3\right)$$
$$=c_2r_2r_3\dot{\bar{q}}_2+c_2r_2\dot{\bar{t}}_3+r_2q_{20}+r_2\bar{q}_2+r_3q_{20}+r_3\bar{q}_2+t_{30}+\bar{t}_3$$
$$=c_2r_2r_3\dot{\bar{q}}_2+(r_2+r_3)\bar{q}_2+(r_2+r_3)q_{20}+c_2r_2\dot{\bar{t}}_3+\bar{t}_3+t_{30}$$

The equation on $\dot{\bar{t}}_1$:

$$\dot{\bar{t}}_1=c_2r_2r_3\ddot{\bar{q}}_2+(r_2+r_3)\dot{\bar{q}}_2+c_2r_2\ddot{\bar{t}}_2+\dot{\bar{t}}_3$$

The equation on q:

$$q=c_1\dot{t}_1+c_2\dot{t}_2+q_2$$
$$=c_1\left[c_2r_2r_3\ddot{\bar{q}}_2+(r_2+r_3)\dot{\bar{q}}_2+c_2r_2\ddot{\bar{t}}_2+\dot{\bar{t}}_3\right]+c_2\left(r_3\dot{\bar{q}}_2+\dot{\bar{t}}_3\right)+\left(q_{20}+\bar{q}_2\right)$$
$$=c_1c_2r_2r_3\ddot{\bar{q}}_2+(c_1r_2+c_1r_3+c_2r_3)\dot{\bar{q}}_2+\bar{q}_2+q_{20}+c_1c_2r_2\ddot{\bar{t}}_2+(c_1+c_2)\dot{\bar{t}}_3$$

The equation on t:

$$t=r_1q+r_2q_1+r_3q_2+t_3$$
$$=r_1\left[c_1c_2r_2r_3\ddot{\bar{q}}_2+(c_1r_2+c_1r_3+c_2r_3)\dot{\bar{q}}_2+\bar{q}_2+q_{20}+c_1c_2r_2\ddot{\bar{t}}_2+(c_1+c_2)\dot{\bar{t}}_3\right]$$
$$+r_2\left(c_2r_3\dot{\bar{q}}_2+c_2\dot{\bar{t}}_3+q_{20}+\bar{q}_2\right)+r_3\left(q_{20}+\bar{q}_2\right)+t_{30}+\bar{t}_3$$
$$=\begin{bmatrix}c_1c_2r_1r_2r_3\ddot{\bar{q}}_2+\left(c_1r_1r_2+c_1r_1r_3+c_2r_1r_3\right)\dot{\bar{q}}_2+r_1\bar{q}_2+r_1q_{20}\\+c_1c_2r_1r_2\ddot{\bar{t}}_2+(c_1r_1+c_2r_1)\dot{\bar{t}}_3\end{bmatrix}$$
$$+\left(c_2r_2r_3\dot{\bar{q}}_2+c_2r_2\dot{\bar{t}}_3+r_2q_{20}+r_2\bar{q}_2\right)+\left(r_3q_{20}+r_3\bar{q}_2\right)+t_{30}+\bar{t}_3$$
$$=c_1c_2r_1r_2r_3\ddot{\bar{q}}_2+\left(c_1r_1r_2+c_1r_1r_3+c_2r_1r_3+c_2r_2r_3\right)\dot{\bar{q}}_2$$
$$+(r_1+r_2+r_3)\bar{q}_2+(r_1+r_2+r_3)q_{20}+c_1c_2r_1r_2\ddot{\bar{t}}_2+(c_1r_1+c_2r_1+c_2r_2)\dot{\bar{t}}_3+\bar{t}_3+t_{30}$$
$$=b_1\ddot{\bar{q}}_2+b_2\dot{\bar{q}}_2+b_3\bar{q}_2+b_4q_{20}+a_1\ddot{\bar{t}}_2+a_2\dot{\bar{t}}_3+a_3\bar{t}_3+a_4t_{30}$$

Equation for images:

$$(a_1s^2+a_2s+a_3)T_3(s)=-(b_1s^2+b_2s+b_3)Q_2(s)$$

Coefficients:

$$a_1=c_1c_2r_1r_2$$
$$a_2=c_1r_1+c_2r_1+c_2r_2$$
$$a_3=1$$
$$b_1=c_1c_2r_1r_2r_3$$
$$b_2=c_1r_1r_2+c_1r_1r_3+c_2r_1r_3+c_2r_2r_3$$
$$b_3=r_1+r_2+r_3$$

Complex resistance $Z(s)$:

$$Z(s)=\frac{T_3(s)}{Q_2(s)}=\frac{-b_1s^2-b_2s-b_3}{a_1s^2+a_2s+a_3}$$

Frequency function of the circuit:

$$s\to j\Omega,\ j^2=-1$$

Frequency function of the circuit:

$$Z(s)=\frac{T_3(s)}{Q_2(s)}$$

Т. 10. №6. 2024
https://doi.org/10.33619/2414-2948/103

$$=\frac{-b_1s^2-b_2s-b_3}{a_1s^2+a_2s+a_3}=\frac{b_1\Omega^2-b_2j\Omega-b_3}{-a_1\Omega^2+a_2j\Omega+a_3}$$

$$=\frac{\left(b_1\Omega^2-b_2j\Omega-b_3\right)\left[\left(-a_1\Omega^2+a_3\right)-a_2j\Omega\right]}{\left[\left(-a_1\Omega^2+a_3\right)+a_2j\Omega\right]\left[\left(-a_1\Omega^2+a_3\right)-a_2j\Omega\right]}$$

$$=\frac{\begin{pmatrix}-a_1b_1\Omega^4+a_3b_1\Omega^2-a_2b_1j\Omega^3+a_1b_2j\Omega^3-a_3b_2j\Omega-a_2b_2\Omega^2\\+a_1b_3\Omega^2-a_3b_3+a_2b_3j\Omega\end{pmatrix}}{\left(-a_1\Omega^2+a_3\right)^2+a_2^2\Omega^2}$$

$$=\frac{\left[\begin{matrix}-a_1b_1\Omega^4+(a_1b_2-a_2b_1)j\Omega^3+(a_3b_1-a_2b_2+a_1b_3)\Omega^2+\\(a_2b_3-a_3b_2)j\Omega-a_3b_3\end{matrix}\right]}{\left(-a_1\Omega^2+a_3\right)^2+a_2^2\Omega^2}$$

We derive the real part of the complex resistance:

$$Re(j\Omega)=\frac{-a_1b_1\Omega^4+(a_3b_1-a_2b_2+a_1b_3)\Omega^2-a_3b_3}{(-a_1\Omega^2+a_3)^2+a_2^2\Omega^2}$$

We derive the imaginary part of the complex resistance:

$$Im(j\Omega)=\frac{(a_1b_2-a_2b_1)\Omega^3+(a_2b_3-a_3b_2)\Omega}{(-a_1\Omega^2+a_3)^2+a_2^2\Omega^2}j$$

We obtain the amplitude-frequency function of the energy circuit:

$$A(j\Omega)=\sqrt{Re(j\Omega)^2+Im(j\Omega)^2}$$

Get the phase-frequency function of the energy circuit:

$$\varphi(j\Omega)=-arctg\frac{Im(j\Omega)}{Re(j\Omega)}$$

Results and discussion

Parameter are calculated or found from the experiment, for example n_0= 60 W, as well as the inlet pressure P_0= 150 kPa.

The known conditions: P – pressure, kPa; V – volume flow, *l/s* [liter per second]; r_1 – active resistances, $\left[\frac{kPa\cdot s^2}{lit}\right]$; m,m_2 – mass of liquid, [*kg*]; l – hydraulic compliance, $\left[\frac{lit\cdot s}{kPa}\right]$, 1 litre = 10^{-3}metre.

Table 1

CIRCUIT PARAMETERS

m, *kg*	m_2, *kg*	r, $[\frac{kPa\cdot s^2}{lit}]$	l_1,$[\frac{lis\cdot s}{kPa}]$	P_{30}, *kPa*	V_{10}, *lit/s*
12	12	93.75	0.00444	150	0.4
18	12	93.75	0.00444	150	0.4
12	12	93.75	0.00629	150	0.4

Т. 10. №6. 2024
https://doi.org/10.33619/2414-2948/103

Dependency graphs are plotted based on the input values. For the best perception of graphs values are taken only those that affect the dependence. The values obtained for the first stage of the energy circuit are shown in Table 2.

Table 2

RECEIVED INFORMATION FOR HYDRAULIC

Ω	*AjΩ*1	*φjΩ*1	*AjΩ*2	*φjΩ*2	*AjΩ*3	*φjΩ*3
1	275.041526	-0.750104	270.682726	-0.765216	164.345188	-0.607048
2	396.641095	-1.238939	389.483437	-1.297230	197.795467	-1.2467315
3	562.575643	-1.554397	564.279213	1.491364	286.971351	1.3707782
4	766.622090	1.362176	792.092283	1.243327	437.330389	1.0303425
5	1009.63477	1.19049	1074.38113	1.060490	643.60155	0.8158718
6	1293.69942	1.054390	1412.89239	0.921052	901.917905	0.6734301
7	1620.68779	0.943881	1808.90035	0.8118753	1210.36714	0.5730422
8	1992.01669	0.852618	2263.24137	0.724506	1568.01695	0.4987306
9	2408.70151	0.776216	2776.45242	0.653274	1974.38635	0.4415573
10	2871.45787	0.71151	3348.88041	0.594251	2429.21090	0.3962133

Based on the results of the calculation, the graphs of the amplitude frequency response and phase-frequency response and frequency response of the circuit are constructed. Further in these graphs are under construction:

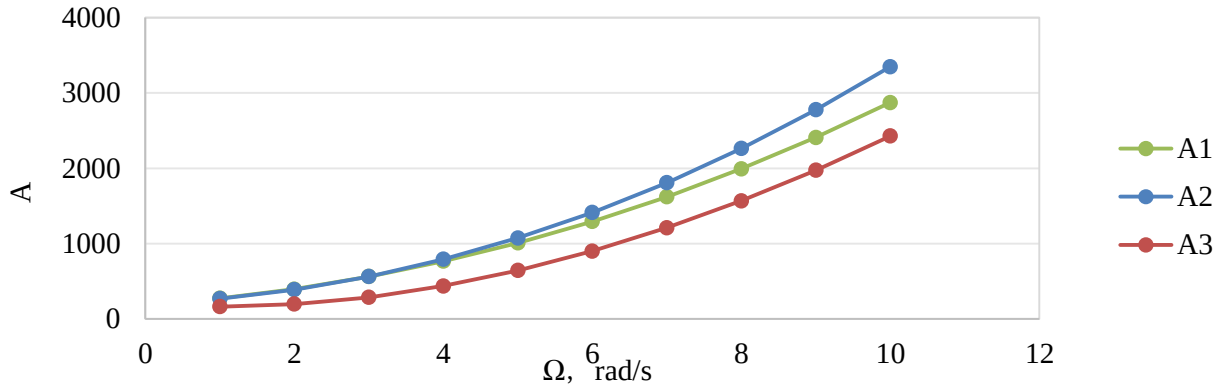

Figure 7. Amplitude frequency response

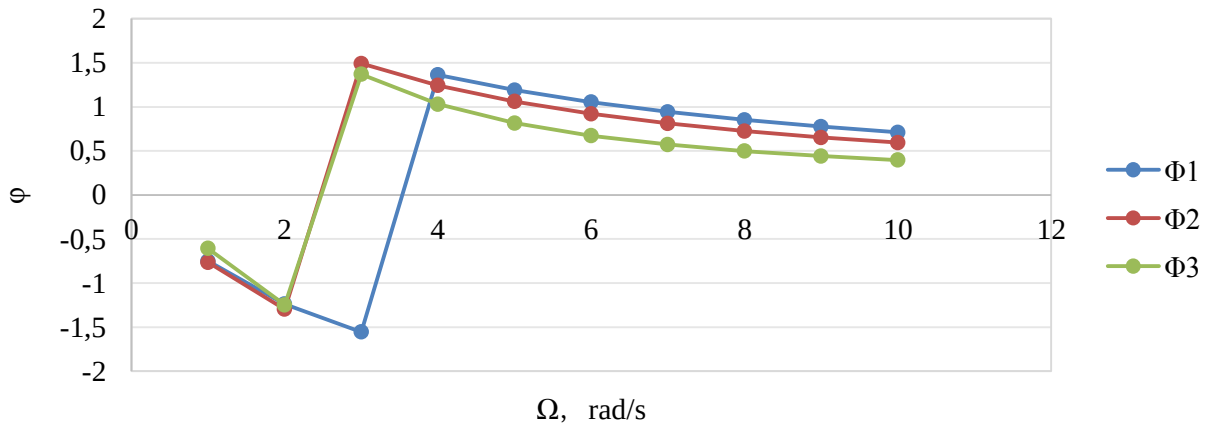

Figure 8. Phase frequency response

Т. 10. №6. 2024
https://doi.org/10.33619/2414-2948/103

When m and l_1 change, the three lines are similar. For A, changing m can reach the maximum at the earliest. For Φ, when these two parameters are changed, the curve fluctuates larger.

For power circuits of the heat transfer calculations are conducted similarly and are written in Table 3. A graphical view is presented in Figure 4-5.

Table 3

RECEIVED INFORMATION FOR HEAT TRANSFER

$r_1, \left[\frac{kPa \cdot s^2}{lit}\right]$	$r_2, \left[\frac{kPa \cdot s^2}{lit}\right]$	$r_3, \left[\frac{kPa \cdot s^2}{lit}\right]$	$c_1, \left[\frac{l}{s \cdot ℃}\right]$	$c_2, \left[\frac{l}{s \cdot ℃}\right]$	$t_0, ℃$	$n_0, \ kW$
0.01	2.17×10^{-5}	2.5×10^{-4}	0.0204	0.0204	70	25
0.02	2.17×10^{-5}	2.5×10^{-4}	0.0204	0.0204	70	25
0.01	2.17×10^{-5}	2.5×10^{-4}	0.0156	0.0156	80	25

The dependency graph is drawn based on input values. For optimal graph perception, take only those values that affect dependencies. The obtained values for the first stage of heat transfer are shown in Table 3.

Table 4

VALUE AMPLITUDE FREQUENCY RESPONSE FOR ENERGY CIRCUIT

Ω	$Aj\Omega1$	$\varphi j\Omega1$	$Aj\Omega2$	$\varphi j\Omega2$	$Aj\Omega3$	$\varphi j\Omega3$
1	0.010271699	0.000398071	0.020271693	0.000805937	0.010271699	0.000304407
2	0.010271697	0.000796141	0.020271673	0.001611873	0.010271698	0.000608814
3	0.010271692	0.001194212	0.020271639	0.002417807	0.010271695	0.000913221
4	0.010271686	0.001592282	0.020271592	0.003223737	0.010271692	0.001217627
5	0.010271679	0.001990351	0.020271531	0.004029663	0.010271687	0.001522034
6	0.010271669	0.00238842	0.020271457	0.004835584	0.010271682	0.00182644
7	0.010271658	0.002786487	0.020271369	0.005641498	0.010271675	0.002130846
8	0.010271645	0.003184554	0.020271268	0.006447405	0.010271668	0.002435251
9	0.010271631	0.00358262	0.020271153	0.007253302	0.010271659	0.002739656
10	0.010271614	0.003980685	0.020271025	0.00805919	0.01027165	0.00304406

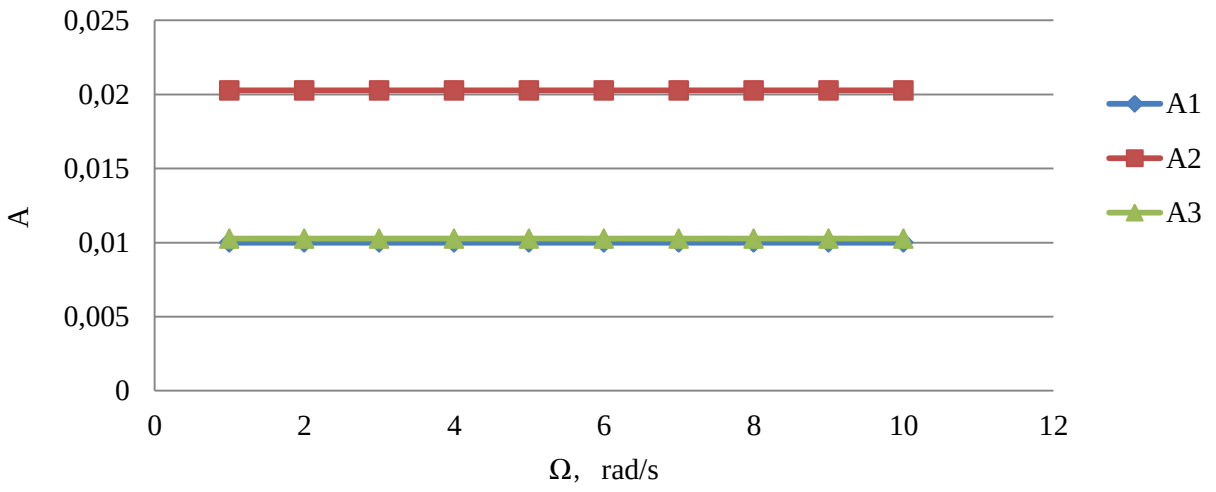

Figure 9. Amplitude frequency response

Т. 10. №6. 2024
https://doi.org/10.33619/2414-2948/103

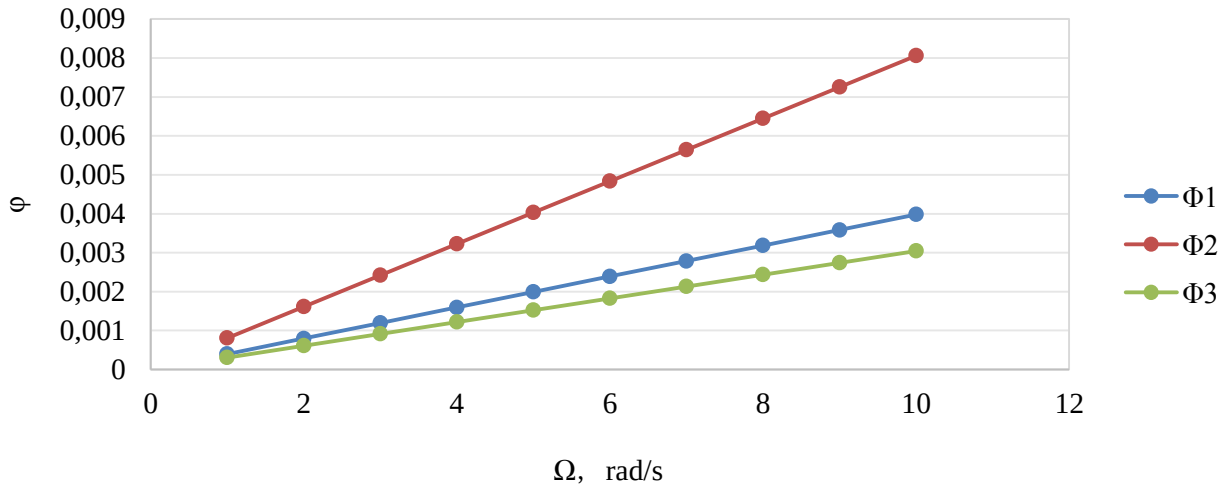

Figure 10. Phase frequency response

When r_1 and t_0 change, the curve trend is similar. Judging from the above two pictures, changing r_1 has the greatest impact on A and Φ. r_1 becomes bigger, A and Φ also become larger.

Conclusions

In this paper, the problems associated with this work and possible solutions are described. A constructive scheme of the experimental device is proposed and the principle of its operation is described in detail. The power circuit of the device is drawn up, each link is explained. Complex impedance, frequency function, amplitude-frequency characteristic and phase-frequency characteristic are obtained by mathematical transformation of the power circuit. The frequency response of the circuit is constructed.

The description of the experimental setup is completed, energy circuits for hydraulics and heat transfer are compiled.

Energy circuits in hydraulics take into account such parameters as pressure, volume flow, hydraulic losses, hydraulic resistance, hydraulic mass. Energy circuits for heat transfer take into account such parameters as the mass flow rate of the medium, temperature, thermal resistance, thermal power.

In the process of modeling the hydraulic power circuit, it is found that with the increase of frequency, the frequency response of the hydraulic circuit increases and quickly reaches the optimal value, and the amplitude will decrease. As the frequency increase, the PFC of the hydraulic circuit drops.

In the process of modeling the heat transfer of the energy circuit, it is found that the frequency response of the hydraulic circuit decreases with the increase of frequency, producing a uniform pulsation.

According to the resulting graphs, one can trace the relationship between two different properties. It can be seen from the graph that for a particular r value, we reach the frequency maximum faster.

References:

1. Zhu, Zhifu. (2005). An effective way to utilize automobile waste heat. *Journal of Heilongjiang Institute of Engineering (Natural Science Edition), 19*(2), 51-53.

2. Rowe, M. (2009). An overview of thermoelectric waste heat recovery activities in Europe. *Thermoelectrics applications workshop, San Diego,* 34-48.

3. Delgado, O., & Lutsey, N. (2014). The US SuperTruck Program. *Washington DC*.

4. Teng, H., Klaver, J., Park, T., Hunter, G. L., & van der Velde, B. (2011). *A rankine cycle system for recovering waste heat from HD diesel engines-WHR system development* (No. 2011-01-0311). SAE Technical Paper. https://doi.org/10.4271/2011-01-0311.

5. Horst, T. A., Rottengruber, H. S., Seifert, M., & Ringler, J. (2013). Dynamic heat exchanger model for performance prediction and control system design of automotive waste heat recovery systems. *Applied Energy*, *105*, 293-303. https://doi.org/10.1016/j.apenergy.2012.12.060

6. Wang, E. H., Zhang, H. G., Zhao, Y., Fan, B. Y., Wu, Y. T., & Mu, Q. H. (2012). Performance analysis of a novel system combining a dual loop organic Rankine cycle (ORC) with a gasoline engine. *Energy*, *43*(1), 385-395. https://doi.org/10.1016/j.energy.2012.04.006

7. Khaliq, A., & Trivedi, S. K. (2012). Second law assessment of a wet ethanol fuelled HCCI engine combined with organic Rankine cycle. https://doi.org/10.1115/1.4005698

8. Tahani, M., Javan, S., & Biglari, M. (2013). A comprehensive study on waste heat recovery from internal combustion engines using organic Rankine cycle. *Thermal Science*, *17*(2), 611-624. https://doi.org/10.2298/TSCI111219051T

9. Kim, Y. M., Shin, D. G., Kim, C. G., & Cho, G. B. (2016). Single-loop organic Rankine cycles for engine waste heat recovery using both low-and high-temperature heat sources. *Energy*, *96*, 482-494. https://doi.org/10.1016/j.energy.2015.12.092

10. Rijpkema, J., Munch, K., & Andersson, S. B. (2018). Thermodynamic potential of twelve working fluids in Rankine and flash cycles for waste heat recovery in heavy duty diesel engines. *Energy*, *160*, 996-1007. https://doi.org/10.1016/j.energy.2018.07.003

11. Jing, Guohui, & Fan, Jianxin (2010). Overview of the technical development of the total energy utilization system of marine diesel engines. *Diesel engine, 32*(6), 1-4.

12. Ichiki, Y. O., Shiraishi, K. E., Kanaboshi, T. A., Ono, Y. O., & Ohta, Y. U. (2011). Development of super waste-heat recovery system for marine diesel engines. *Mitsubishi Heavy Ind Tech Rev*, *48*(1), 17-21.

13. Sun, Lizhu (2014). Modeling and Simulation of Residual Heat Utilization System for Marine Diesel Engines. *Harbin University of Technology,* 3.

Список литературы:

1. Zhu Zhifu. An effective way to utilize automobile waste heat // Journal of Heilongjiang Institute of Engineering (Natural Science Edition). 2005. V. 19. №2. P. 51-53.

2. Rowe M. An overview of thermoelectric waste heat recovery activities in Europe // Thermoelectrics applications workshop. 2009. P. 34-48.

3. Delgado O., Lutsey N. The US SuperTruck Program // Washington DC. 2014.

4. Teng H., Klaver J., Park T., Hunter G. L., van der Velde B.A rankine cycle system for recovering waste heat from HD diesel engines-WHR system development. SAE Technical Paper, 2011. №2011-01-0311. https://doi.org/10.4271/2011-01-0311.

5. Horst T. A., Rottengruber H. S., Seifert M., Ringler J. Dynamic heat exchanger model for performance prediction and control system design of automotive waste heat recovery systems // Applied Energy. 2013. V. 105. P. 293-303. https://doi.org/10.1016/j.apenergy.2012.12.060

6. Wang E. H., Zhang H. G., Zhao Y., Fan B. Y., Wu Y. T., Mu Q. H. Performance analysis of a novel system combining a dual loop organic Rankine cycle (ORC) with a gasoline engine // Energy. 2012. V. 43. №1. P. 385-395. https://doi.org/10.1016/j.energy.2012.04.006

7. Khaliq A., Trivedi S. K. Second law assessment of a wet ethanol fuelled HCCI engine combined with organic Rankine cycle. 2012. https://doi.org/10.1115/1.4005698

8. Tahani M., Javan S., Biglari M. A comprehensive study on waste heat recovery from internal combustion engines using organic Rankine cycle // Thermal Science. 2013. V. 17. №2. P. 611-624. https://doi.org/10.2298/TSCI111219051T

9. Kim Y. M., Shin D. G., Kim C. G., Cho G. B. Single-loop organic Rankine cycles for engine waste heat recovery using both low-and high-temperature heat sources // Energy. 2016. V. 96. P. 482-494. https://doi.org/10.1016/j.energy.2015.12.092

10. Rijpkema J., Munch K., Andersson S. B. Thermodynamic potential of twelve working fluids in Rankine and flash cycles for waste heat recovery in heavy duty diesel engines // Energy. 2018. V. 160. P. 996-1007. https://doi.org/10.1016/j.energy.2018.07.003

11. Jing Guohui, Fan Jianxin. Overview of the technical development of the total energy utilization system of marine diesel engines // Diesel engine. 2010. V. 32. №6. P. 1-4.

12. Ichiki Y. O., Shiraishi K. E., Kanaboshi T. A., Ono Y. O., Ohta Y. U. Development of super waste-heat recovery system for marine diesel engines // Mitsubishi Heavy Ind Tech Rev. 2011. V. 48. №1. P. 17-21.

13. Sun Lizhu. Modeling and Simulation of Residual Heat Utilization System for Marine Diesel Engines // Harbin University of Technology. 2014. P. 3.

Работа поступила
в редакцию 28.04.2024 г.

Принята к публикации
04.05.2024 г.

Ссылка для цитирования:

Zhou Min, Kuznetsov D. The Energy Circuit of the Exhaust Gas Heat Recovery Circuit of a 25 kW Diesel Generator // Бюллетень науки и практики. 2024. Т. 10. №6. С. 317-329. https://doi.org/10.33619/2414-2948/103/35

Cite as (APA):

Zhou, Min, & Kuznetsov, D. (2024). The Energy Circuit of the Exhaust Gas Heat Recovery Circuit of a 25 kW Diesel Generator. *Bulletin of Science and Practice, 10*(6), 317-329. https://doi.org/10.33619/2414-2948/103/35